The 2017 World Congress on
Advances in Structural Engineering and Mechanics (ASEM17)
28 August - 1 September, 2017, Ilsan(Seoul), Korea

Iterative coupling of precise integration FEM and TD-BEM for elastodynamic analysis

Weidong Lei[1)], Chun Liu[2)], Hongjun Li[3)], *Xiaofei Qin[4)] and Rui Chen[5)]

[1),2) ,4) ,5)]*Shenzhen Graduate School, Harbin institute of Technology, Shenzhen, 518055, China*
[3)]*Hualan Design & Consulting Group, Nanning, 530011, China*
[4)] *270113745@qq.com*

ABSTRACT

The iterative coupling formulation of the precise integration finite element method (FEM) and the time domain boundary element method (TD-BEM) is presented for elstodynamic problems. In the formulation, the FEM node and the BEM node are not required to be coincident on the common interface between FEM and BEM sub-domains, therefore, the FEM and BEM are independently discretized. The force and displacement converting matrices are used to transfer data between FEM and BEM nodes on the common interface between the FEM and BEM sub-domains, to renew the nodal variables in the process of the iterations for the un-coincident FEM node and BEM node. The iterative coupling formulation for elastodynamics in current paper is of high modeling accuracy, due to the semi-analytical solution incorporated in the precise integration finite element method. The iterative coupling for elastodynamics is verified by examples of a cantilever bar under a Heaviside-type force and a harmonic load.
Key words: the iterative coupling; elstodynamic; the finite element method, the boundary element method

1. Introduction

During the past decades, both the finite element method (FEM) and the boundary element method (BEM) have been extensively studied to handle a wide range of engineering problems, each with its own advantages and disadvantages. However, the practical engineering problems are so complicated that in some cases it is desirable to combine FEM and BEM together to enhance their advantages and weaken their disadvantages. The coupling formulations of FEM and BEM naturally emerged in the process of the evolution of the numerical formulations. At the first time Zienkiewicz and

---

[1) ,5)] Associate Professor
[2) ,3) ,4)] Graduate Student

Kelly (1977) proposed the coupling formulation of FEM and BEM. In the coupling method, the governing equations of FEM and BEM formulations were established for FEM sub-domain and BEM sub-domain respectively, based on which the unified governing equation for the whole domain was further established to realize the compatibility between FEM and BEM formulations. Subsequently, a lot of contributions to the conventional coupling formulations were made by authors of several literatures (Brebbia 1980, Li at al. 1986, Leung at al. 1995, Estorff and Prabucki 1990, Yu 2001). It has been found that the conventional coupling formulation with the unified governing equation was applicable for static and elastodynamic problems, however, the numerical implementation of the coupling in the whole domain was quiet complex for some cases, due to the matrix operations between the symmetrical and sparsely populated FEM matrix and the fully populated BEM matrix, resulting in weakening the advantages in FEM and BEM formulations. Therefore, Prasad (1992) proposed the domain decomposition coupling formulation of FEM and BEM, in which it was not required to the combine the FEM and BEM governing equations, and the discretizations and solutions of the FEM and BEM sub-domains were independently conducted. Lin and Lawton (1996) published the domain decomposition coupling formulation, in which the iteration of nodal variables between FEM and BEM formulations on the common interface between FEM and BEM sub-domains were performed till the convergence to obtain the real values of the nodal variables on the common interface. After that the FEM and BEM sub-domains were independently solved in their own frames. Elleithy & Al-Gahtani (2000) and Elleithy *et al.* (2001) proposed the over lapping domain decomposition coupling formulation for some special boundaries and summarized three kinds of domain decomposition coupling approaches. Later, Elleithy and Tanaka (2003,2004) studied the convergence and the relaxation parameter for the over lapping domain decomposition coupling formulation in other three literatures. Cifuentes *et al.* (2015) successfully applied numerical simulation of the coupled dynamic response of a submerged floating tunnel with mooring lines to regular waves. Yan *et al.* (2006) proposed an improved domain decomposition coupling formulation, in which the FEM and BEM were not required to be discretized at the coincident nodes on the common interface between the FEM and BEM sub-domains, hence to release the freedom for the discretization of the sub-domains. Based on the time domain BEM formulation (TD-BEM, with TD for time domain), Soare Jr proposed a special domain decomposition coupling formulation of FEM and TD-BEM, in which different durations for each time step in BEM and FEM sub-domains were allowed in the analysis (Soares *et al.* 2004, Soares 2008, Soares 2012, Soares *et al.* 2015). Lu *et al.* (2015) researched time-domain analyses of the layered soil by the modified scaled boundary finite element method.Therefore, the consistence of the coupling formulation was improved. Moreover, the coupling formulation was applicable in dynamic problems both for elastic and inelastic analysis. Later on, the study on relaxation parameter was carried out for inelastic dynamic analysis in the process of the coupling. Comparing the domain decomposition coupling formulation against the conventional coupling formulation of the unified equation in the whole domain, the domain decomposition coupling formulation has its obvious advantages. First, the order of the coefficients matrix is reduced, that is, the computational cost is lower. Second, the duration of time steps is more flexible, hence the computation is more versatile and consistent. Moreover, in the frame of the domain

decomposition coupling formulation, the iterative coupling mechanism can be independently coded case by case for the common interface between the FEM and BEM sub-domains, while the FEM and the BEM sub-domains can be independently modeled in their own formulations, even directly transplanting some standard modules. However, in the process of the treatment to the FEM governing equation under the frame of the domain decomposition coupling formulation, Wilson-θ and Newmark approaches were often employed to handle the time differential terms in the original FEM governing equation by means of the finite difference, supposing the linear variation for the nodal acceleration. The approximation in the treatment of the finite difference to the terms in the dynamic equation of motion, relevant to time, might undermine the modeling accuracy. Zhong and Williams (1994) proposed the precise integration FEM, in which the analytical solution of the equation of motion in terms of time was obtained by treating the second-ordered differential equations with the method of decreasing the order, and the integration in terms space was numerically solved by FEM. Therefore, the precise integration FEM is a semi-analytical solution, with better modeling accuracy comparing with the pure numerical solution.

In current paper, a coupling formulation of the precise integration FEM and the TD-BEM is proposed. In the formulation, the semi-analytical scheme is incorporated to improve the modeling accuracy in the standard domain decomposition coupling formulation. Meanwhile, it has been noticed that in the standard domain decomposition coupling formulation, it is required that the FEM and BEM nodes on the common interface between the two sub-domains share the coincident positions. However, when the FEM and BEM sub-domains are independently discretized under their own formulations, the FEM and BEM nodes on the common interface might not be positioned on the same positions. In current coupling formulation, the nodal information on different positions between FEM and BEM sub-domains are transferred by the force converting and displacement converting matrices. Therefore, it is not required the coincident positions for the FEM and BEM nodes on the common interface, i.e., besides being more accurate, the current coupling formulation on the other hand is more versatile and manipulated.A cantilever bar subjected to two independent loads, one for a Heaviside-type force the other one for a harmonic load, is considered to verify the coupling method in this paper.

2. Force and displacement converting matrices

In classical domain decomposition coupling formulation, the domain of the original problem is divided into FEM and BEM sub-domains, which are independently discretized. The force and displacement on the artificial common interface between FEM and BEM sub-domains are unknown. The solution of the unknowns on the common interface between the two sub-domains has the first priority in the frame of the coupling formulation. Upon those interfacial unknowns are solved, the problems for the corresponding sub-domains become the independent FEM and BEM problems.

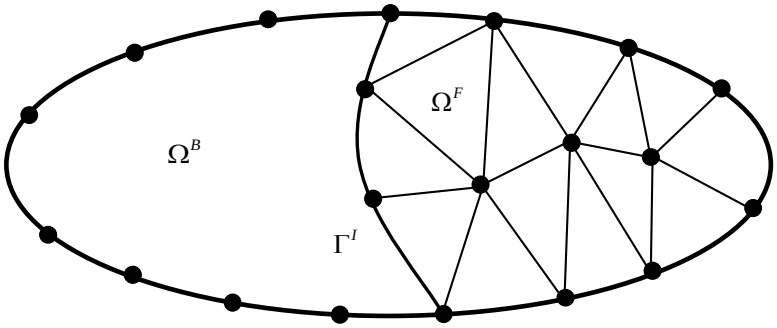

Fig. 1 Domain decomposition

As shown in Fig.1, the stressed elastic and continuous body is divided into FEM sub-domain Ω^F and BEM sub-domain Ω^B. The common interface between FEM and BEM sub-domain is Γ^I. The BEM and FEM sub-domains are discretized using one dimensional linear boundary elements and two dimensional plane elements respectively.

Upon discretization of the boundary integral equation for the BEM sub-domain, the following BEM governing equation is obtained:

$$Hu_B = Gp_B \tag{1}$$

where, H, G, u_B and p_B are the coefficient matrix of nodal displacement, the coefficient matrix of nodal traction, the vector of nodal displacement and the vector of nodal traction, respectively, for the BEM sub-domain.

Similarly, the FEM governing equation can also be obtained, as:

$$Ku_F = f_F \tag{2}$$

where K, u_F and f_F are the global stiffness matrix, the nodal displacement vector and the equivalent nodal force vector, respectively, for the FEM sub-domain.

Separating the nodal variables in the governing equations of BEM and FEM systems in Eq.s (1) and (2) by the nodal variables of the common boundary and the remaining domain, where the common boundary is not included, Eq.s (1) and (2) become the following sub-structured forms, in Eq.s (3) and (4) respectively, as:

$$\begin{bmatrix} K_{11} & K_{12} \\ K_{21} & K_{22} \end{bmatrix} \begin{bmatrix} u_F^F \\ u_F^I \end{bmatrix} = \begin{bmatrix} f_F^F \\ f_F^I \end{bmatrix} \tag{3}$$

$$\begin{bmatrix} H_{11} & H_{12} \\ H_{21} & H_{22} \end{bmatrix} \begin{bmatrix} u_B^B \\ u_B^I \end{bmatrix} = \begin{bmatrix} G_{11} & G_{12} \\ G_{21} & G_{22} \end{bmatrix} \begin{bmatrix} p_B^B \\ p_B^I \end{bmatrix} \tag{4}$$

where, in Eq. (3), u_F^F, u_F^I, f_F^F and f_F^I stand for the following vectors:

u_F^F : the displacement vector of the nodal in the external FEM sub-domain, where the common boundary is not included,

u_F^I : the displacement vector of the nodal on the interface between FEM and BEM sub-domains, approached from FEM sub-domain,

f_F^F : the equivalent force vector of the nodal on the external FEM sub-domain, where the common boundary is not included,

f_F^I : the equivalent force vector of the nodal on the interface between FEM and BEM sub-domains, approached from FEM sub-domain;

and where, in Eq. (4), u_B^B, u_B^I, p_B^B and p_B^I respectively represent for the following vectors:

u_B^B: the displacement vector of the nodal on the external boundary in the BEM sub-domain,

u_B^I: the displacement vector of the nodal on the interface between FEM and BEM sub-domains,

p_B^B : the traction vector of the nodal on the external boundary in the BEM sub-domain,

p_B^I: the traction vector of the nodal on the interface between FEM and BEM sub-domains.

In order to incorporate the FEM and BEM sub-domains in the coupling system, the forces and the displacements of the nodes on the interface from FEM and BEM formulations are required to satisfy certain conditions. In the case where the FEM nodes on the interface are coincident with the BEM nodes, the equivalent forces of nodes from the FEM sub-domain and tractions of the nodes from the BEM sub-domain are required to satisfy the equilibrium equation, and the corresponding displacements are required to satisfy the compatibility condition (Yan *et al.* 2006).

The equilibrium equation is expressed by the nodal forces, as:

$$f_F^I + Mp_B^I = 0 \tag{5}$$

where M is the converting matrix, expressed by $M = \int_\Gamma N^T N d\Gamma$, and N is the interpolation function for node on the interface approached from BEM sub-domain, which is coincident with the position of the node approached from FEM sub-domain.

The compatibility condition is expressed by the nodal displacements, as:

$$u_B^I = u_F^I \tag{6}$$

From Eq.s (5) and (6), it can be seen that it is required that the position of the FEM node is coincident with the BEM node on the interface between FEM and BEM sub-domains. The position requirement bounds the discretization of the two sub-domains. Moreover, the corner treatment is complicated, so that the nonconforming boundary element is necessary for the discretization. For details of nonconforming boundary element, literature (Song and Nie 2009) is referred. Therefore, the coupling system allowing the different node positions between FEM and BEM

sub-domain is more flexible and meaningful than the coupling system of the coincident nodes.

In current paper, the force and displacement converting matrices are used to transfer data between FEM and BEM nodes on the interface, to realize the renewal of the nodal variables in the process of the iterations for the case where the FEM and BEM nodes are located at different positions. The traction of the FEM node on the interface can be obtained from the traction of the BEM node on the interface by means of interpolation, as:

$$p_B^{IF} = N_B p_B^I \tag{7}$$

where p_B^{IF} is traction vector of node on the interface approached from BEM sub-domain, which is coincident with the position of the node approached from FEM sub-domain, and N_B is the matrix of interpolation functions for the boundary element.

In the following context, the mechanism of the information transmission between FEM and BEM variables for the nodes on the interface is illustrated by a conceptual coupling example, where the eight-node isoparameteric finite elements are coupled with linear nonconforming boundary elements. By the way, in the example, the difference between ***N*** and N_B is also illustrated.

In a supposing case, where the eight-node isoparameteric finite element and linear nonconforming boundary element are employed to discretize the FEM and BEM sub-domains respectively, the relationship between the nodal traction and nodal equivalent force on the common interface between FEM and BEM sub-domains is shown in Fig. 2. p_1 and p_2 are the nodal tractions in BEM sub-domain, while f_1, f_2 and f_3 are the nodal equivalent forces in FEM sub-domain. Applying the principle of virtual work to solve the force transmission for the nodes on the interface between FEM and BEM systems, it is required that the nodes of the two systems are coincident. Therefore, the two BEM nodes with the tractions p_1 and p_2 are transferred to three artificial BEM nodes with tractions p_1^F, p_2^F and p_3^F on the interface, which are coincident with the corresponding positions of the three nodes approached from FEM sub-domain.

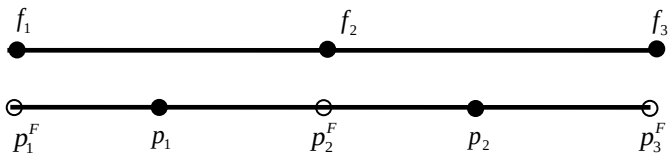

Fig. 2 The relationship between forces of FEM and BEM sub-domains

In the example, in order to discretize the two internal BEM nodes with the tractions p_1 and p_2 to the boundary, the following interpolation or extrapolatopn function is used:

$$N_B = \left[\frac{1}{2} - \xi \qquad \frac{1}{2} + \xi \right] \tag{8}$$

where ξ is the coordinate value in natural coordinate system.

Discretizing the three BEM nodes with the tractions p_1^F, p_2^F and p_3^F, which are coincident with the three corresponding FEM nodes, to the boundary, the following interpolation or extrapolation function is used:

$$N = \left[\frac{(\xi - 1)\xi}{2} \qquad 1 - \xi^2 \qquad \frac{(\xi + 1)\xi}{2} \right] \tag{9}$$

By interpolating the displacements of the FEM nodes on the interface, the displacements of the FEM nodes, coincident with the positions of the corresponding BEM nodes, can be obtained, as:

$$u_F^{IB} = N_F u_F^I \tag{10}$$

where N_F is for the FEM interpolation function.

In the case where the FEM nodes on the interface are not coincident with the BEM nodes, the equivalent forces in FEM system and the tractions in BEM system satisfy the following equilibrium condition:

$$f_F^I + M p_B^{IF} = 0 \tag{11}$$

Displacement coordination condition for the BEM nodes is expressed, as:

$$u_B^I = u_F^{IB} \tag{12}$$

By considering Eq.s (7) and (11), one has:

$$f_F^I = -M N_B p_B^I \tag{13}$$

Therefore, the converting matrix for transforming nodal tractions in BEM system to nodal equivalent forces in FEM system is as follows:

$$Tr\_F = -M N_B \tag{14}$$

By considering Eq.s (10) and (12), one has:

$$u_B^I = N_F u_F^I \tag{15}$$

Therefore, the converting matrix for transforming nodal displacements in FEM system to BEM system is as follows:

$$Tr\_U = N_F \tag{16}$$

For the conceptual coupling example, the force and the displacement converting matrices can be quantitatively expressed. As shown in Fig. 2, the force is often transformed from BEM system to FEM system. Then, p_1 and p_2 are known, therefore, the traction of arbitrary point on the linear nonconforming boundary element is:

$$p = (\frac{1}{2} - \xi) p_1 + (\frac{1}{2} + \xi) p_2 \tag{17}$$

By giving -1, 0 and 1 to ξ respectively, one has:

$$\begin{cases} p_1^F = \frac{3}{2} p_1 - \frac{1}{2} p_2 \\ p_2^F = \frac{1}{2} p_1 + \frac{1}{2} p_2 \\ p_3^F = -\frac{1}{2} p_1 + \frac{3}{2} p_2 \end{cases} \tag{18}$$

or, in matrix format, as:

$$\begin{bmatrix} p_1^F \\ p_2^F \\ p_3^F \end{bmatrix} = \begin{bmatrix} \frac{3}{2} & -\frac{1}{2} \\ \frac{1}{2} & \frac{1}{2} \\ -\frac{1}{2} & \frac{3}{2} \end{bmatrix} \begin{bmatrix} p_1 \\ p_2 \end{bmatrix} \tag{19}$$

Then, the matrix of the interpolation functions N_B in Eq. (7) is:

$$N_B = \begin{bmatrix} \frac{3}{2} & -\frac{1}{2} \\ \frac{1}{2} & \frac{1}{2} \\ -\frac{1}{2} & \frac{3}{2} \end{bmatrix} \tag{20}$$

For plane problems, the converting matrix is expressed, as:

$$M = \int_L N^T N dl = \int_L \begin{bmatrix} N_1 \\ N_2 \\ N_3 \end{bmatrix} \begin{bmatrix} N_1 & N_2 & N_3 \end{bmatrix} dl = \frac{L}{30} \begin{bmatrix} 4 & 2 & -1 \\ 2 & 16 & 2 \\ -1 & 2 & 4 \end{bmatrix} \tag{21}$$

Recalling Eq. (14), the quantitative force converting matrix from BEM system to FEM system for the conceptual coupling example is as follows:

$$Tr\_F = \frac{L}{12} \begin{bmatrix} -3 & 1 \\ -4 & -4 \\ 1 & -3 \end{bmatrix} \tag{22}$$

In the conceptual coupling example, the displacement of arbitrary point in the eight-node isoparameteric finite element, as shown in Fig. 3, can be expressed by the

displacements of the nodes.

The displacement for point *a* in Fig. 3 is $u_a = \sum_{i=1}^{8} N_i u_i$, and ξ in the interpolation function N_i is either 1 or 1/2. Then one has:

$$u_a = -\frac{1}{8}u_2 + \frac{3}{8}u_3 + \frac{3}{4}u_6 \tag{23}$$

Similarly, for point *b* in Fig. 3, one has:

$$u_b = \frac{3}{8}u_2 - \frac{1}{8}u_3 + \frac{3}{4}u_6 \tag{24}$$

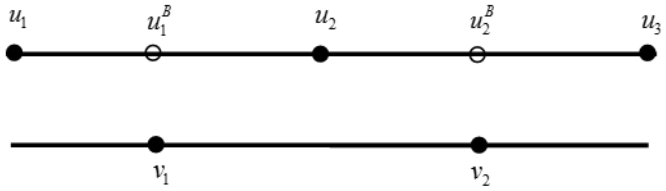

Fig. 4 The relationship between displacements of FEM and BEM sub-domains

The relationship between nodal displacements for FEM and BEM systems are shown in Fig. 4. v_1 and v_2 are the nodal displacements in BEM system, and u_1, u_2 and u_3 are the nodal displacements in FEM system. u_1^B and u_2^B are the displacements of the nodes in FEM system, which are coincident with the positions of the nodes in the BEM system.

The displacement is often transformed from FEM system to BEM system. When u_1, u_2 and u_3 are known, according to Eq.s (23) and (24), one has:

$$\begin{bmatrix} u_1^B \\ u_2^B \end{bmatrix} = \begin{bmatrix} \frac{3}{8} & \frac{3}{4} & -\frac{1}{8} \\ -\frac{1}{8} & \frac{3}{4} & \frac{3}{8} \end{bmatrix} \begin{bmatrix} u_1 \\ u_2 \\ u_3 \end{bmatrix} \tag{25}$$

Because displacements of the node in FEM system the node in BEM system are the same, one has:

$$\begin{bmatrix} v_1 \\ v_2 \end{bmatrix} = \begin{bmatrix} u_1^B \\ u_2^B \end{bmatrix} \tag{26}$$

Therefore, the quantitative displacement converting matrix from FEM system to BEM system for the conceptual coupling example is as follows:

$$Tr\_U = \frac{1}{8}\begin{bmatrix} 3 & 6 & -1 \\ -1 & 6 & 3 \end{bmatrix} \tag{27}$$

3. Coupling of precise integration BEM and TD-BEM

The equation of motion can be solved by both the direct numerical integration method and the mode combination method. In the direct integration method, the numerical integration is directly conducted before the integration of the equation of motion, without transformation operation in the equation set. By contrast, in the mode combination method, the decoupling needs to be done in the equation set by using the orthogonality between the stiffness and the mass matrices. The mode combination method is not applicable for the inelasticity. The conventional direct numerical integration method includes central difference method, Wilson-θ method and Newmark method. In the three direct integration methods, the difference discretization is conducted in the computation, and the linear acceleration is assumed for the nodes, undermining the modeling accuracy.

By adopting the treatment of the order reduction to the second-ordered differential equation, in the precise integration method, the analytical expression of the equation of motion in terms of time variable is obtained, while the discretization in space is performed by employing finite elements. Therefore, this semi-analytical method is of higher modeling accuracy comparing with the numerical solution.

Treating the displacement of the particle of the elastic body as an unknown, the equation of motion is expressed, as:

$$M\ddot{x} + C\dot{x} + Kx = f(t) \tag{28}$$

where M , C and K respectively represent for the mass matrix, the damping matrix, stiffness matrix， and x , $\dot{x}$ and $\ddot{x}$ for the displacement, the velocity and the acceleration of the particle.

By introducing the transformation $y = M\dot{x} + Cx/2$, order of the equation of motion is deduced by one, and the analytical expression in terms of time is obtained . For more details, interested readers can refer literatures (Zhong and Williams 1994, Wang and Zhou 2005). The general solution to non-homogenous equation for elastodynamic problem is obtained as follows:

$$v(t) = e^{Ht}v_0 + \int_0^t e^{H(t-\tau)}r(\tau)d\tau \tag{29}$$

In Eq. (29), $v = \begin{Bmatrix} x \\ y \end{Bmatrix}$, $r(\tau) = \begin{bmatrix} 0 \\ f(\tau) \end{bmatrix}$. $e^{\boldsymbol{H}t}$ is coefficient matrix. The matrix *H* is expressed as： $H = \begin{bmatrix} -M^{-1}C/2 & M^{-1} \\ CM^{-1}C/4 - K & -CM^{-1}/2 \end{bmatrix}$.

Therefore, the recursion relationship for two adjacent time steps can be expressed,

as:

$$v_{n+1} = Tv_n + \int_{n\Delta t}^{(n+1)\Delta t} e^{H[(n+1)\Delta t-\tau]} r(\tau) d\tau \tag{30}$$

where $T = e^{H\Delta t}$.

The governing equation of elastodynamics for TD-BEM is:

$$H^n u^n = G^n p^n + B^n \tag{31}$$

where H^n, G^n, u^n and p^n stand for the displacement influencing coefficient matrix, the traction influencing coefficient matrix, the vector of nodal displacement and the vector of nodal traction, with the superscript *n* for the nth time step.

The governing equation, Eq. (30), for elastodynamics for FEM can be written, as:

$$u^{n+1} = Tu^n + R^n \tag{32}$$

where $u^n = v_n$, $R^n = \int_{n\Delta t}^{(n+1)\Delta t} e^{H[(n+1)\Delta t-\tau]} r(\tau) d\tau$.

To describe the iterative process of coupling of the precise integration FEM and TD-BEM, notations of the vectors of displacement and force for the nodes on the common interface and the remaining FEM and BEM sub-domains are defined, where u, f and p are conventionally used to specify the displacement, the equivalent nodal force and the traction, and different superscripts and subscripts are also used for detailed specifications. u_F^n and f_F^n respectively stand for the displacement and equivalent force at the nth time step for the nodes on the remaining FEM sub-domain except the interface, where the superscript *n* and the subscript *F* respectively represent for the nth time step and the remaining FEM sub-domain except the interface. Similarly, u_B^n and p_B^n are the displacement and the traction at the nth time step foe the nodes on the entire external boundary of the BEM sub-domain. u_{FI}^n, f_{FI}^n, u_{BI}^n and p_{BI}^n are for the displacement and the force at the nth time step for the nodes on the common interface, respectively approached from the FEM sub-domain (denoted by the subscript *FI*) and BEM sub-domain (denoted by the subscript *BI*). $u_{FI(k)}^n$, $f_{FI(k)}^n$, $u_{BI(k)}^n$ and $p_{BI(k)}^n$ are for the displacement and the force at the kth iteration (donated by the subscript in the parentheses) at the nth time step for the nodes on the common interface.

Taking the computation of the displacement and the force at the nth time step as an example to illustrate how the computation in Eq.s (31) and (32) is carried out. In this scenario, in the BEM frame, the displacement and the traction before the nth time step are known, so, B^n is also known. Therefore, the coefficient matrices H^n and G^n in Eq. (31) can be obtained. In the FEM frame in Eq. (32), when the exponent matrix T is known, the equivalent force at the nodes at the (n+1)th time step on the common interface can be obtained by linear interpolation, based on the corresponding equivalent

force at the n[th] time step. When f_{FI}^{n} and f_{FI}^{n+1} are known, in the duration $n\Delta t \sim (n+1)\Delta t$, the value of $r(\tau)$ can be obtained, and the corresponding integration R^n can be solved.

The proposed iterative coupling method for the (n+1)[th] time step can be described as follows:

(1) Based on the calculated displacement and force at the end of the n[th] time step, i.e., u_F^n, u_{FI}^n, u_B^n, u_{BI}^n, f_F^n, f_{FI}^n, p_B^n and p_{BI}^n are known,

(2) According to Eq. (32), and supposing $f_{FI(0)}^{n+1} = f_{FI}^{n}$, all the nodal displacements $u_{F(0)}^{n+1}$ and $u_{FI(0)}^{n+1}$ can be calculated.

(3) By using the displacement converting matrix Eq. (16), $u_{BI(0)}^{n+1}$ can be obtained.

(4) Combining the boundary condition p_B^{n+1}, $p_{BI(0)}^{n+1}$ and $u_{B(0)}^{n+1}$ can be calculated according to the governing equation for BEM in Eq. (31)

(5) $f_{FI(1)}^{n+1}$ is obtained, based on $p_{BI(0)}^{n+1}$ and the force converting matrix Eq. (14).

(6) Checking if $f_{FI(k)}^{n+1}$ and $f_{FI(k+1)}^{n+1}$ satisfy the convergence condition $\| f_{FI(k+1)}^{n+1} - f_{FI(k)}^{n+1} \| / \| f_{FI(k+1)}^{n+1} \| \leq \varepsilon$ or not , where ε is the given tolerance. If the convergence is satisfied, treating $f_{FI(k+1)}^{n+1}$ as the real nodal equivalent force at the common interface approached from FEM sub-domain, go back to the loop from step (2)-(5) to solve the problem, finalizing the computation for (n+1)[th] time step. If convergence has not been achieved, go to step (7).

(7) Set $f_{FI(k+1)}^{n+1} = (1-\omega) f_{FI(k)}^{n+1} + \omega f_{FI(k+1)}^{n+1}$, where ω is the relaxation parameter, and go to the loop from steps (2)-(6), until two results are closed enough. Then the computation goes to the next time step.

It is noted that the key is step (1), that is the initial conditions of displacement and the force for the computation for the (n+1)[th] time step. Further back to $n = 0$, the initial conditions are given, i.e., u_F^0, u_B^0, f_F^0 and p_B^0 are known, and generally the initial conditions on the common interface u_{FI}^0 and u_{BI}^0 are also known. The equivalent nodal force on the interface approached from FEM sub-domain and the nodal traction on the interface from BEM sub-domain are more complicated. In the case where the common interface is initially stressed, the equivalent nodal force and the nodal traction are unknown. Nevertheless, the trial initial equivalent nodal force and the traction can be given 0.

4. Numerical examples

4.1 Statement of the problem

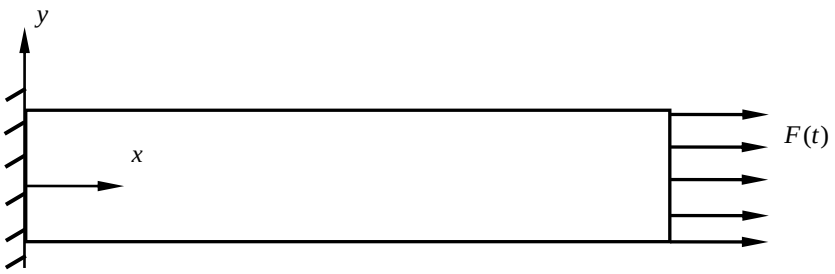

Fig. 5 Geometry of a rod and distribution of the load

As shown in Fig.5, the left end of the rod is fixed, while the right end is free. The geometries of the rod are: $\text{length}\, l = 1\ \text{m}$, $\text{width}\, b = 0.1\ \text{m}$ and $\text{thcikness}\, h = 0.1\ \text{m}$. The load is normally imposed at the free end on the right along x-axis. The motion state of the rod is described by the horizontal displacement *u*. Two loads are independently applied to specify two numerical examples, one for a Heaviside-type force the other one for a harmonic load, as shown in Fig. 6 (a) and (b) respectively.

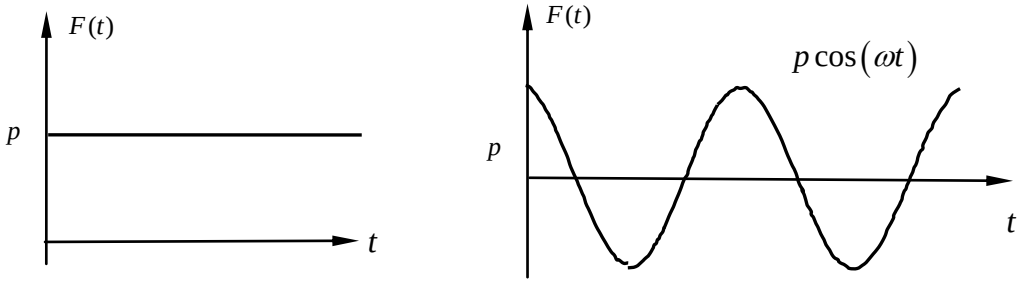

(a) Heaviside-type load (b) Harmonic load

Fig. 6 The external loads

In the verification example, the material parameters of the rod are: the elastic modulus *E*=2000 Pa and the mass density *ρ*=2000 kg/m^3. So, the velocity of the P wave is calculated as, *C*=1 m/s. The external pressure P (or the wave amplitude) is $p = 1000\ \text{MPa}$, and circular frequency of the harmonic wave is $\omega = \pi$.

4.2 The analytical solution

The axial displacement of the cantilever bar can be expressed by one dimensional wave equation, as:

$$\frac{\partial^2 u}{\partial t^2} = c^2 \frac{\partial^2 u}{\partial x^2} \tag{33}$$

where the wave velocity is $c = \sqrt{E/\rho}$, and the corresponding initial condition is as

follows:

$$u|_{t=0} = u_t|_{t=0} = 0 \tag{34}$$

The corresponding boundary condition is:

$$\begin{cases} u|_{x=0} = 0 \\ u_x|_{x=l} = p/E \end{cases} \tag{35}$$

The analytical solution of the axial displacement of the cantilever bar is:

$$u = \frac{p}{E}x + \sum_{n=1}^{\infty} \frac{(-1)^n 8pl}{(2n-1)^2 \pi^2 E} \cos\frac{(2n-1)\pi c}{2l} t \sin\frac{(2n-1)\pi}{2l} x \tag{36}$$

According to Fourier series, a periodic load is composited by infinite harmonic loads with different frequencies. In the two numerical examples in current research, one for the Heaviside-type load $F = p$ and the other for the harmonic load $F = p\cos(\omega t)$, if the circular frequency ω approaches 0, one has $F = p$. To the authors' best knowledge, the analytical solution of the axial displacement of the cantilever bar under harmonic load is not available, which is supposed to derive in current research. By considering the relationship between these two loads, it is obvious that the example of the Heaviside-type load is a special example of the harmonic load. While the axial displacement of the cantilever bar under the Heaviside-type load is given, it can be used to validate the proposed analytical solution under the condition, the circular frequency ω approaching 0.

By introducing the notation $v = u - Fx/E = u - \frac{p\cos(\omega t)}{E}x$, the wave equation Eq. (33) is written, as:

$$\begin{cases} \frac{\partial^2 v}{\partial t^2} = c^2 \frac{\partial^2 v}{\partial x^2} + f(x,t) \end{cases} \tag{37}$$

The initial condition Eq. (34) is expressed, as:

where $f(x,t) = \frac{p\omega^2 \cos(\omega t)}{E}x$.

$$\begin{cases} v|_{t=0} = u|_{t=0} - \frac{p}{E}x = -\frac{p}{E}x \\ v_t|_{t=0} = u_t|_{t=0} = 0 \end{cases} \tag{38}$$

The boundary condition Eq. (35) is expressed, as:

$$\begin{cases} v|_{x=0} = u|_{x=0} = 0 \\ v_x|_{x=l} = u_x|_{x=l} - \frac{p\cos(\omega t)}{E} = 0 \end{cases} \tag{39}$$

Supposing $v(x,t) = w_1(x,t) + w_2(x,t)$, the initial equation Eq. (37) is changed into the follows, as:

$$\begin{cases} \dfrac{\partial^2 w_1}{\partial t^2} = c^2 \dfrac{\partial^2 w_1}{\partial x^2} \\ w_1(0,t) = 0, \dfrac{\partial w_1}{\partial x}(l,t) = 0 \\ w_1(x,0) = -\dfrac{p}{E}x, \dfrac{\partial w_1}{\partial t}(x,0) = 0 \end{cases} \tag{40}$$

$$\begin{cases} \dfrac{\partial^2 w_2}{\partial t^2} = c^2 \dfrac{\partial^2 w_2}{\partial x^2} + f(x,t) \\ w_2(0,t) = 0, \dfrac{\partial w_2}{\partial x}(l,t) = 0 \\ w_2(x,0) = 0, \dfrac{\partial w_2}{\partial t}(x,0) = 0 \end{cases} \tag{41}$$

Eq. (40) is a homogeneous partial differential equation, one can obtain the follows:

$$w_1 = \sum_{n=1}^{\infty} (-1)^n \frac{2p}{k^2 El} \cos(kct) \sin(kx) \tag{42}$$

where $k = \dfrac{2n-1}{2l}\pi$.

For the convenience in expression, replacing w_2 with w, and supposing $w = w_n \sin(kx)$, after that, by solving Eq. (41), one has:

$$\begin{aligned} \sum_{n=1}^{\infty} w_n''(t)\sin(kx) &= \sum_{n=1}^{\infty} (-k^2c^2) w_n(t)\sin(kx) + f(x,t) \\ &= \sum_{n=1}^{\infty} (-k^2c^2) w_n(t)\sin(kx) + \sum_{n=1}^{\infty} f_n(t)\sin(kx) \end{aligned} \tag{43}$$

In Eq. (43), by considering $f(x,t) = \sum_{n=1}^{\infty} f_n(t)\sin(kx)$, one has:

$$f_n(t) = \frac{2}{l}\int_0^l f(x,t)\sin(kx)dx = (-1)^{n+1} \frac{2p\omega^2 \cos(\omega t)}{k^2 El} \tag{44}$$

By simplifying Eq. (43), one has:

$$w_n'' + c^2 k^2 w_n = f_n(t) \tag{45}$$

The corresponding initial condition is expressed, as:

$$\begin{cases} w_n(0) = 0 \\ w_n^{'}(0) = 0 \end{cases} \tag{46}$$

Fourier transformation is performed to Eq. (45), one has:

$$\begin{cases} w_n^{''}(t) \to p^2 w_n(p) - p w_n(0) - w_n^{'}(0) = p^2 w_n(p) \\ w_n(t) \to w_n(p) \\ f_n(t) \to F_n(p) \end{cases} \tag{47}$$

Putting Eq. (47) into Eq. (45), one has:

$$p^2 w_n(p) + c^2 k^2 w_n(p) = F_n(p) \tag{48}$$

By solving Eq. (48), one can obtain the following:

$$w_n(p) = \frac{1}{p^2 + c^2 k^2} F_n(p) \tag{49}$$

According to Fourier transformation, one has:

$$\frac{1}{p^2 + c^2 k^2} \to \frac{1}{kc} \sin(kct) \tag{50}$$

Eq. (49) can be changed into the following equation by means of Fourier transformation, as:

$$w_n(t) = \frac{1}{kc} \sin(kct) \otimes f_n(t) = \frac{1}{kc} \int_0^t f_n(\tau) \sin[kc(t-\tau)] d\tau \tag{51}$$

where $\otimes$ is the notation for convolution.

Putting Eq. (44) into Eq. (51), the following equation is obtained, as:

$$w = \sum_{n=1}^{\infty} (-1)^{n+1} \frac{2p\omega^2}{k^3 Elc} \int_0^t \cos(\omega\tau) \sin[kc(t-\tau)] d\tau \tag{52}$$

Therefore, the analytical solution to the axial displacement of the cantilever bar under the harmonic load is expressed, as:

$$\begin{aligned} u = {} & \frac{p\cos(\omega t)}{E} x + \sum_{n=1}^{\infty} (-1)^n \frac{2p}{k^2 El} \cos(kct) \sin(kx) \\ & + \sum_{n=1}^{\infty} (-1)^{n+1} \frac{2p\omega^2}{k^3 Elc} \int_0^t \cos(\omega\tau) \sin[kc(t-\tau)] d\tau \end{aligned} \tag{53}$$

The integral term in Eq. (53) can be expressed by the following expressions for three cases:

$$\int_0^t \cos(\omega\tau) \sin[kc(t-\tau)] d\tau = -t \sin(\omega t)/2 \qquad \text{case 1: } \omega = -ck$$

$$\int_0^t \cos(\omega\tau)\sin[kc(t-\tau)]d\tau = t\sin(\omega t)/2 \qquad \text{case 2: } \omega = ck \text{ and } \omega \neq 0$$

$$\int_0^t \cos(\omega\tau)\sin[kc(t-\tau)]d\tau = \frac{ck[\cos(kct)-\cos(\omega t)]}{\omega^2 - k^2c^2} \qquad \text{case 3: } \omega \text{ for other other values}$$

When $\omega = 0$, it is found that Eq. (53) is the same as Eq. (36), that is the derived analytical solution to the axial displacement of the cantilever bar under harmonic load at special condition of $\omega = 0$ is the same as that under the Heaviside-type load. It validate from a certain viewpoint that the derivation in current research is correct.

4.3 Numerical treatment

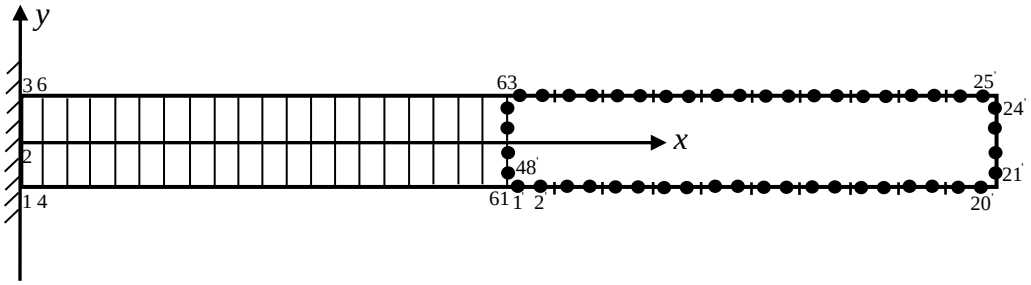

Fig. 7 Discretization of the cantilever bar

The domain of the cantilever bar is divided into two sub-domains. The sub-domain close to the fixed end is discretized with finite elements by employing plane four-node elements, while the free end sub-domain is discretized with boundary elements by employing the linear 1/4 symmetrical non-conforming boundary elements with 2 nodes. The common interface is at the middle of the bar. The FEM sub-domain is discretized into 40 finite elements with 63 nodes, while the BEM sub-domain is discrteized into 24 boundary elements with 48 nodes, as shown in Fig. 7.

The FEM and BEM sub-domains are independently numbered. In the FEM sub-domain, the nodes and the finite elements are numbered in the sequence of from bottom to top and from left to right. In the BEM sub-domain, the boundary elements and nodes are numbered anti clockwise.

4.4 Comparison between numerical and analytical results

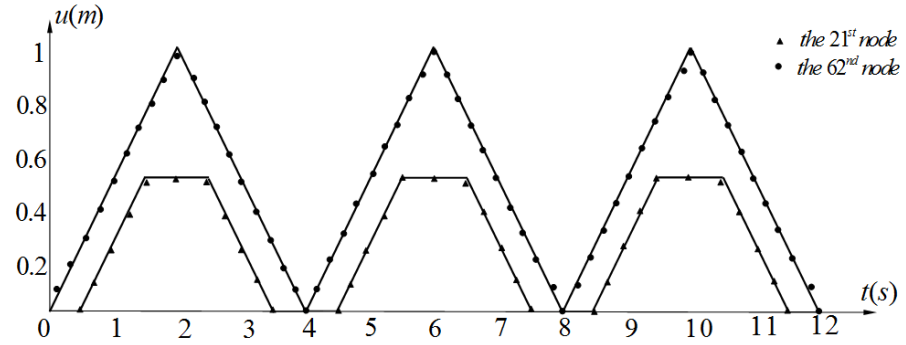

Fig. 8 Comparison between the results in terms of the axial displacement from the proposed coupled formulation and the analytical solution for the case of Heaviside-type load

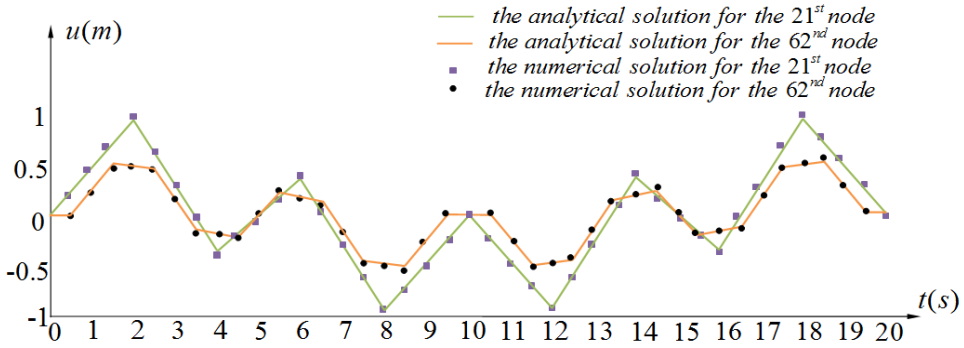

Fig. 9 Comparison between the results in terms of the axial displacement from the proposed coupled formulation and the analytical solution for the case of harmonic load

Tow representative nodes, the 21st boundary element node （1，-0.0375） at the free end and the 62nd finite element node （0.5，0） at the middle of the bar, are chosen for the comparison. Fig. 8 shows the time histories from the coupled formulation of the axial displacements of the two chosen FEM and BEM nodes for the case of the Heaviside-type load, and Fig. 9 shows those for the case of the harmonic load. For the comparison purpose, the analytical results from Eq. (36) for the two chosen nodes are included in Fig. 8, and those from Eq. (53) are included in Fig. 9. In the two figures, the sparse dots stand for the results from the coupled formulation, while the continuous lines stand for those from analytical solutions.

From Fig.s 8-9, it can be seen that the results from the coupling formulation of precise integration FEM and BEM well agree with those from the analytical solutions, for different points under different loads in a long term. It indicates that the proposed force and displacement converting matrices are correct, and it also indicates that the proposed coupling formulation of precise integration FEM and BEM is correct, accurate and consistent.

5. Conclusions

The main findings can be summarized as follows:

- The iterative coupling formulation of the precise integration FEM and TD-BEM is proposed for dynamic problems. The coupling formulation is verified to be correct by a cantilever bar under Heaviside-type and harmonic transient loads, with good modeling accuracy and consistence.
- The force and displacement converting matrices are proposed to transfer the nodal information on different positions between FEM and BEM sub-domains. It is not required the coincident positions for the FEM and BEM nodes on the common interface between FEM and BEM sub-domains. Therefore, the coupling formulation is versatile and easily manipulated.
- Based on the analytical expression of the equation of motion in time and the discretization in space by finite elements, the precise integration FEM formulation is a semi-analytical method, with good modeling accuracy comparing with pure numerical solution. Moreover, in the proposed coupling formulation of the precise integration FEM and TD-BEM, the finite difference treatment to the time differential terms in the original FEM governing equation is evaded, where the modeling error might be accumulated. Therefore the proposed coupling formulation of the precise integration FEM and BEM is accurate.
- The analytical solution of a cantilever bar under harmonic transient load is derived. On one hand, the solution is used to verify the proposed coupling formulation of the precise integration FEM and TD-BEM. On the other hand, the good agreement between the results from the proposed coupling formulation and the derived analytical solution indicates, to a certain degree, that the derivation procedure is correct.

Acknowledgments

The authors would like to acknowledge the financial support from the research grant, No. JCYJ20140417172417171 provided by Shenzhen Science and Technology Planning Program.

References

Brebbia, C.A. (1980), *Boundary Element Techniques In Engineering*, Pentech Press, London, Britain.

Cifuentes, C., Kim, S., Kim, M.H. and Park. W.S. (2015), “Numerical simulation of the coupled dynamic response of a submerged floating tunnel with mooring lines in regular waves”, *Struct. Eng. Mech.,* **5**(2), 109-123.

Elleithy, W.M. and Al-Gahtani, H.J. (2000), “An overlapping domain decomposition approach for coupling the finite and boundary element methods”, *Eng. Anal. Bound. Elem*., **24**(5), 391–398.

Elleithy, W.M., Al-Gahtani, H.J. and El-Gebeily, M. (2001), "Iterative coupling of BE and FE methods in elastostatics", *Eng. Anal. Bound. Elem*., **25**(8),685-695.

Elleithy, W.M. and Tanaka, M. (2003), "Interface relaxation algorithms for BEM–BEM coupling and FEM–BEM coupling", *Comput. Meth. Appl. Mech. Eng*., **192**(26–27), 2977-2992.

Elleithy, W.M. and Tanaka, M. (2004), "A Guzik interface relaxation FEM–BEM coupling method for elasto-plasticanalysis", *Eng. Anal. Bound. Elem*., **28**(7), 849-857.

Estorff, O. von and Prabucki, M.J. (1990), "Dynamic response in the time domain by coupled boundary and finite elements", *Comput. Mech*., **6**(1), 35–46.

Leung, K.L., Zavareh, P.B. and Beskos, D.E. (1995), "2D elastostatic analysis by a symmetric BEM/FEM scheme", *Eng. Anal. Bound. Elem*., **15**(1), 67–78.

Li, H.B., Han, G.M., Mang, H.A. and Torzicky, P. (1986), "A new method for the coupling of the finite element and boundary element discretized subdomains of elastic bodies", *Comput. Meth. Appl. Mech. Eng*., **54**(2), 161–185.

Lin, C.C. and Lawton, E.C. (1996), "An iterative finite element-boundary element algorithm", *Comput. Struct*., **59**(5), 899-909.

Lu, S., Liu, J., Lin G. and Wang W.Y. (2015), "Time-domain analyses of the layered soil by the modified scaled boundary finite element method", *Struct. Eng. Mech.,* **55**(5), 1055-1086.

Prasad, N.N.V. (1992), "Integrated techniques for coupled elastostatic BEM and FEM analysis", M. eng. Thesis; The University of New Mexico, Albuquerque, USA.

Soares, D. (2008), "An optimised FEM-BEM time-domain iterative coupling algorithm for dynamic analyses", *Comput. Struct*., **86**(19-20), 1839-1844.

Soares, D. (2012), "FEM-BEM iterative coupling procedures to analyze interacting wave propagation models: fluid-fluid, solid-solid and fluid-solid analyses", *Coupled Syst. Mech*., **1**(1), 19-37.

Soares, D., Estorff, O.V. and Mamsur, W.J. (2004), "Iterative coupling of BEM and FEM for nonlinear dynamic analyses", *Comput. Mech*., **34**(1), 67-73.

Soares, D., Goncalves, K.A. and Telles, J.C.D.F. (2015), "Elastodynamic analysis by a frequency-domain FEM-BEM iterative coupling procedure", *Coupled Syst. Mech*., **4**(3), 263-277.

Song, L.F. and Nie, G.H. (2009), "Treatment of corners using discontinuous boundary elelment", *Chin. Q. Mech*., **30**(3), 371-377.

Wang, M.F. and Zhou, X.Y. (2005), "Modified precise time step integration method of structural dynamic analysis", *Earthq. Eng. Eng. Vib*., **4**(2), 287-293.

Yan, B., Du, J., Hu, N. and Sekine, H. (2006), "A domain decomposition algorithm with finite element boundary element coupling", *Appl. Math. Mech*., **27**(4), 519-525.

Yu, G., Mansur, W.J., Carrer, J.A.M. and Lie, S.T. (2001), "A more stable scheme for BEM/FEM coupling applied to two-dimensional elastodynamics", *Comput. Struct*., **79**(8), 811–823.

Zhong, W.X. and Williams, F.W. (1994), "A precise time step integration method", *J. Mech. Eng. Science*., **208**(63), 427-430.

Zienkiewicz, O.C. and Kelly D.W. (1977), "The coupling of the finite element method and boundary solution procedures", *Int. J. Numer. Meth. Eng.,* **11**(2), 355-375.